Diffusion- and Perfusion-Weighted MR Imaging of Dural Sinus Thrombosis

James Manzione, George C. Newman, Avishai Shapiro and Ramon Santo-Ocampo

AJNR Am J Neuroradiol 2000, 21 (1) 68-73
http://www.ajnr.org/content/21/1/68

AJNR Am J Neuroradiol 21:68–73, January 2000

Case Report

Diffusion- and Perfusion-Weighted MR Imaging of Dural Sinus Thrombosis

James Manzione, George C. Newman, Avishai Shapiro, and Ramon Santo-Ocampo

Summary: A patient with dural sinus thrombosis had progressively worsening symptoms and signs that resolved after intradural thrombolysis. Intradural sinus pressures were 54 mm Hg. Echo-planar MR imaging revealed complex abnormalities of diffusion and widespread delay in mean transit time that improved immediately after thrombolysis. This case suggests that diffusion- and perfusion-weighted imaging can provide valuable information noninvasively to help triage patients with dural sinus thrombosis between conservative and aggressive management.

Dural sinus thrombosis (DST) is an uncommon condition with diverse etiologies and protean clinical manifestations, but the diagnosis of DST has been greatly facilitated with the advent of MR imaging (1). Treatment options range from observation to intravenous heparin to intradural thrombolysis (1–5). Currently there are no accepted criteria to help determine when conservative or aggressive treatment of DST would be best; thrombolytics are used primarily in those patients who worsen while on heparin. It would be preferable to be able to predict which patients would be likely to worsen despite heparin administration so that thrombolytic treatment could be initiated before clinical deterioration and to be able to eliminate patients who should not be unnecessarily exposed to the risks of thrombolytic therapy. Our recent experience with diffusion- and perfusion-weighted MR imaging of a patient with DST suggests that these techniques provide significantly more information about the physiologic state of the brain after DST than does conventional MR imaging. These techniques may have the potential to permit triage of patients between conservative therapy with heparin and microcatheter-directed thrombolysis. In this article, we present a single patient with acute sagittal and lateral sinus thrombosis whose symptoms progressed despite heparin administration and in whom diffusion- and perfusion-weighted MR imaging revealed functional deficits considerably beyond the abnormalities shown by conventional MR imaging. The development of the deficits during clinical progression and their regression during clinical improvement suggest that these advanced imaging techniques may be useful in the triage between conservative and aggressive treatment of patients with DST.

Received February 3, 1999; accepted after revision April 1, 1999.

From the Departments of Radiology (J.M., A.S., R.O.) and Neurology (G.C.N.), State University of New York at Stony Brook.

Address reprint requests to James Manzione, MD, Department of Radiology, HSC L4-092, SUNY at Stony Brook, Stony Brook, NY 11794-8460.

Case Report

A 21-year-old right-handed woman awoke one morning with severe frontal headache together with left-hand and left perioral numbness and tingling. She had a 3-year history of migraine and had been taking oral contraceptives for 7 months, but was otherwise healthy. There was no family history of coagulopathy or venous thrombosis. She was admitted to a local hospital. The next morning her headache had worsened; the numbness extended to the elbow and she had left-arm weakness. CT and MR imaging (Fig 1A) revealed thrombosis of the superior sagittal and right transverse dural sinuses. Heparin administration was begun. The next morning she awoke with more severe headache, left-arm numbness to the shoulder, and increased arm weakness with clumsiness. She began to experience focal clonic seizures of the left arm without altered consciousness, initially lasting 10 to 15 seconds, but subsequently persisting for up to 25 minutes despite an intravenous loading dose of phenytoin. MR venography at the regional hospital confirmed prior results, and T2-weighted MR imaging showed apparent infarction in the posterior right frontal lobe (Fig 1B). She was transferred to Stony Brook University Hospital for thrombolytic therapy.

On admission, the patient appeared mildly lethargic and in obvious discomfort from her headache. Her blood pressure was 110/69, her pulse was 62 beats per minute, and her respirations were 18 breaths per minute. There was mild left-gaze paresis and moderate (3/5) left-arm weakness with poor fine-motor coordination. Sensation was moderately reduced from the hand to the shoulder. No seizures were present. Fundoscopic examination revealed mild papilledema without spontaneous venous pulsations. The results of the remainder of the general and neurologic examinations were normal. Initial laboratory tests revealed a fibrinogen of 556 mg/dL. Erythrocyte sedimentation rate and antinuclear antibody, rheumatoid factor, protein S, and activated protein C levels were subsequently normal. Neither anticardiolipin antibodies nor Factor V Leiden were present.

Our standard brain attack protocol was performed on a 1.5-T MR whole-body system using high-performance gradients (peak strength, 27 mT/m) and a standard head coil. After place-

ment of a 3-plane scout localizer, a T2-weighted fast spin-echo axial study of the brain was obtained (3300/96/16 [TR/TE/excitations]; slice thickness, 5 mm; ETL, 4; inter-echo spacing, 11.5 ms; FOV, 24 cm; matrix, 192 × 256). This was followed by a fluid-attenuated inversion-recovery sequence (11975/114/220 [TR/TE/TI]) and echo-planar diffusion-weighted imaging (3000/106 [TR/TE]; FOV, 29.5; slice thickness, 5 mm; inter-echo time, 880 μs; gap, 1 mm; matrix, 119 × 116; flip angle, 90°; and a signal average with fat saturation). Diffusion sensitivity was obtain with two b values (0 and 1000 s/mm^2) taken in three orthogonal directions corresponding to read-, slice-, and phase-encoded directions. The apparent diffusion coefficient was calculated for each pixel from the trace of the three directions. Gradient echo-planar perfusion-weighted images were obtained while manually injecting a double dose of gadolinium through an 18-g angiocatheter placed in an antecubital vein. Each slice was sampled 50 times over the course of 1 minute. The perfusion scanning parameters were as follows: 1200/30 (TR/TE); FOV, 31.5 cm; slice thickness, 7 mm; gap, 3 mm; matrix 127 × 102; flip angle, 90°; and 1 signal average with fat saturation. Images were postprocessed to provide relative regional cerebral blood volume and mean transit time maps.

Diffusion-weighted MR imaging (Fig 1C) showed extensive diffusion abnormalities in the right frontal and parietal lobes. Measurement of the apparent diffusion coefficient, which is not sensitive to the ''T2 shine-through effects,'' revealed normal diffusion in the unaffected left hemisphere and the right prefrontal region and a severe reduction of apparent diffusion coefficient within the right frontal lesion. The severe reduction of apparent diffusion coefficient correlated with the apparent infarction, but a moderate apparent diffusion coefficient reduction in the right parietal region was identified only by diffusion imaging (Table). Perfusion-weighted imaging (Fig 1D) revealed increased relative mean transit time throughout the right cerebral hemisphere, with relatively rapid flow in the region of the left frontotemporal region.

The patient was taken immediately to the angiography suite. A 5F guiding catheter was advanced via a femoral approach into the left internal jugular vein. A Tracker 18 multisided hole-infusion catheter (Target Therapeutics, Freemont, CA) was advanced over a guidewire into the left transverse sinus. The mean venous pressure was 12 mm Hg. Contrast examination showed patency and flow within the left transverse and sigmoid sinuses. The microcatheter was subsequently advanced over the guidewire into the sagittal sinus where the mean pressure was 54 mm Hg. Contrast venography (Fig 1E) confirmed the complete occlusion of the superior sagittal sinus and right transverse sinus. Using a pulse-spray technique, the sagittal sinus was laced with urokinase throughout its course. Approximately 350,000–400,000 units of urokinase were administered and heparin therapy was continued at 1000 U/hr (4–6). Subsequent venography showed partial lysis of the thrombus within the sagittal sinus with establishment of a mild degree of flow. When blood flow was apparent through the superior sagittal sinus, the patient experienced dramatic relief of her headache and spontaneously commented that the numbness of her left hand had begun to lessen. With the infusion catheter in the sagittal sinus, the urokinase infusion was continued at 120,000 U/hr. The patient was examined sequentially over the next few days with progressive repositioning of the microcatheter through the sagittal sinus and subsequently into the right transverse and sigmoid sinuses. After infusion for approximately 3 days, near complete lysis of thrombus was achieved, with excellent restoration of flow through all sinuses (Fig 1F). Mean pressure within the sagittal sinus ranged between 7 and 10 mm Hg. Mean pressure in both transverse sinuses was approximately 5 mm Hg. Clinically, the patient had minimal headache and only a small patch of numbness on the tip of the left thumb by the third day. Repeat diffusion- and perfusion-weighted imaging on the fifth hospital day showed substantial resolution of both the diffusion and perfusion abnormalities (Fig 1G-H, Table). The exception was a persistent diffusion defect and slight prolongation of the index of mean transit time in the region corresponding to the frontoparietal defect seen on the initial T2-weighted and fluid-attenuated inversion-recovery images. Warfarin therapy was initiated at the end of the urokinase infusion. The patient returned to work as an actuarial analyst after 2 weeks and, after 3 months, she was virtually asymptomatic with a stable dose of Coumadin at 15 mg/day. When followed up 1 year later, she was taking no medication, had no recurrence of DST, and only rarely experienced tingling at the tip of her left thumb. Repeat T2-weighted and fluid-attenuated inversion-recovery imaging revealed a very small lesion in the cortex of the post-central gyrus (Fig 1I–J), and diffusion-weighted imaging findings were normal.

Discussion

DST is both uncommon and variable in its clinical course so that controlled treatment trials are difficult to organize. It is estimated that 75% of patients or more will recover completely, without neurologic sequelae (5), but it is also clear that the condition can be fatal (1) or leave patients with seizures and focal neurologic deficits. As a result, recommendations for treatment range from expectant observation, reserving intervention for patients who worsen (7), to aggressive use of thrombolytics (5). This wide range of recommendations reflects the difficulty of predicting the natural history of DST in any single individual. Clinical observation and selection criteria for intervention are helpful but require that the patient be allowed to worsen and, therefore, be exposed to increased risk of chronic sequelae. It appears that intradural sinus pressures can be used to classify patients into five distinct stages that correlate well with clinical findings and conventional imaging results at the time of presentation (1). Because all grade II–IV patients in that study were treated with thrombolysis, the correlation of the initial sinus pressures with subsequent clinical outcome cannot be determined. Furthermore, the disadvantage of intrasinus pressures for patient triage is that it would require dural sinus catheterization in all patients.

Our patient presented with headaches and focal sensory disturbance that progressed clinically over several days, resulting in increased headache and sensory disturbance, weakness, and focal seizures. Imaging studies revealed superior sagittal and right transverse sinus thrombosis. Conventional MR imaging showed focal parenchymal injury that correlated with her neurologic deficits. Direct dural sinus catheterization revealed elevated intradural pressures (54 mm Hg). Diffusion-weighted echo-planar MR imaging prior to thrombolysis revealed parenchymal changes that were much more extensive than those seen with conventional imaging; perfusion-weighted imaging revealed that most of the affected hemisphere had significant alteration of perfusion. She improved promptly and markedly with thrombolysis. Simul-

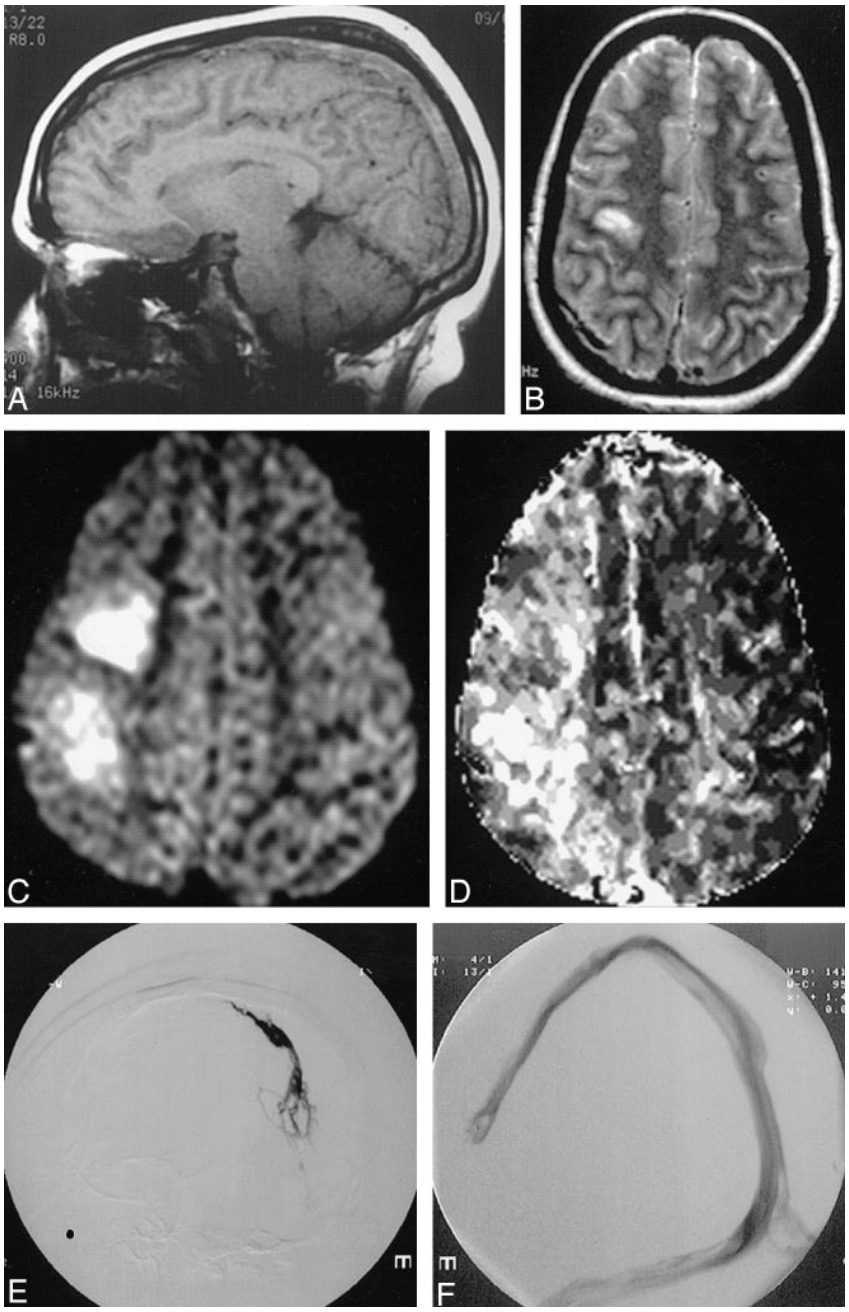

FIG 1. *A,* Sagittal T1-weighted image showing thrombus in the superior sagittal sinus.
B, Axial T2-weighted fast spin-echo image showing small cortical infarct in the posterior frontal lobe.
C, Diffusion-weighted anisotropic image, slice (*z*) direction showing increased signal in the right hemisphere. The denser frontal lesion corresponds to the signal abnormality seen on conventional imaging.
D, Mean transit time map from perfusion-weighted imaging showing a large area of prolonged mean transit time in the right hemisphere.
E, Contrast venography of the sagittal sinus showing venous thrombosis with absent flow.
F, Post-treatment venography showing restoration of flow in the sagittal and transverse sinuses. (cont'd →)

taneously, there was reversal of a significant portion of the diffusion defect and nearly the entire perfusion abnormality. Thus, her course is consistent with the observations that intradural pressures are useful for identifying patients at risk for a poor clinical course (1) and that intradural thrombolysis is a valuable approach to management of progressive disease (1–5). It also suggests, however, that echo-planar MR imaging techniques may allow identification of patients at risk for parenchymal injury while the injury is still reversible. If this is so, then echo-planar MR imaging may prove to be a valuable noninvasive technique for predicting the clinical course of patients and, therefore, for selecting those patients who will benefit from more aggressive management.

Echo-planar MR imaging offers the opportunity to perform both diffusion- and perfusion-weighted

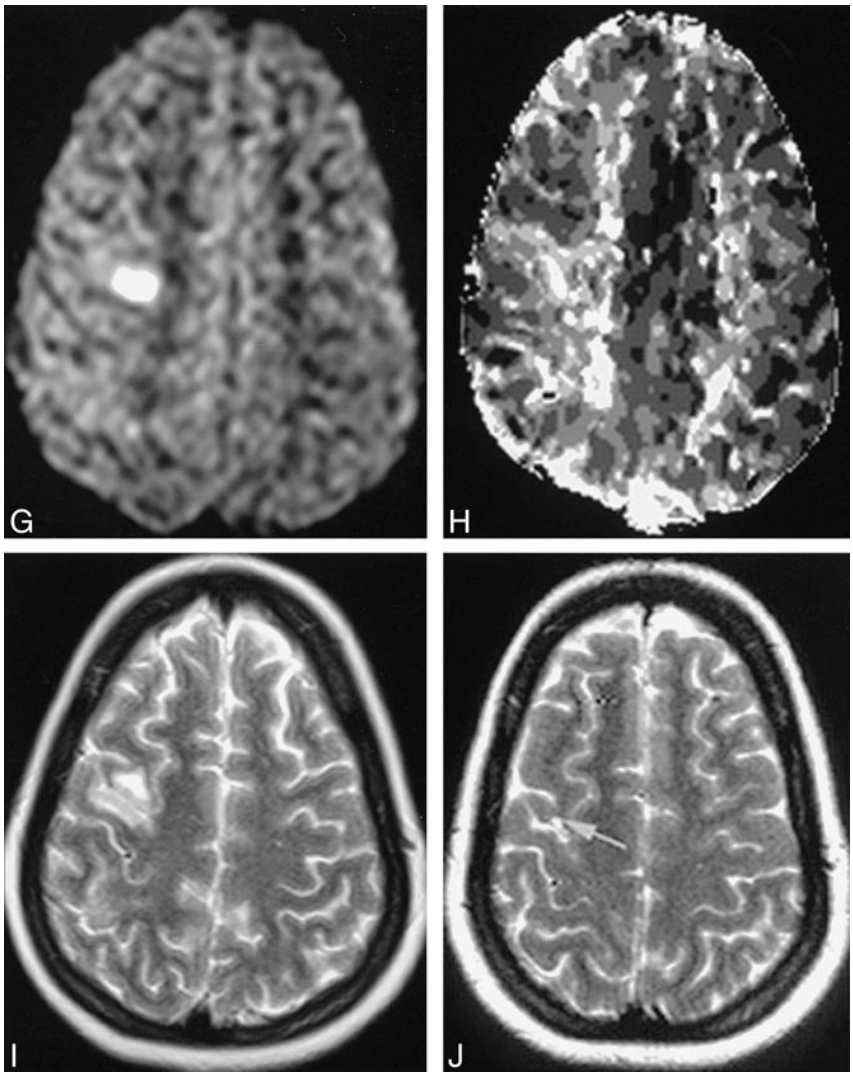

FIG 1. (cont'd) *G,* Post-treatment diffusion-weighted image of the same slice as in *C* showing an area of persistent, although smaller, signal abnormality in the right frontal region and complete resolution of the parietal region defect, presumably representing reversible parenchymal changes of intracellular water accumulation.

H, Post-treatment perfusion-weighted imaging showing marked improvement in the mean transit delay.

I, Post-treatment axial T2-weighted fast spin-echo image unchanged from images prior to treatment. The small cortical infarct persists and no new lesion has developed in the parietal lobe.

J, 1-year follow-up axial T2-weighted fast spin-echo image showing extremely small residual cortical lesion.

imaging. Diffusion-weighted images reflect the random translational motion of water in the brain and provide an estimate and an apparent diffusion coefficient (8). Under ischemic conditions, diffusion-weighted imaging shows slowing of diffusion with increased apparent diffusion coefficient, which is thought to reflect the net transfer of water from the extracellular space, where diffusion is relatively fast, to intracellular spaces, where diffusion of water is more restricted as a result of falling high-energy phosphates (8, 9). The basis of diffusion abnormalities that occur with venous disease is understood less well but may relate to a local increase in transcapillary and interstitial pressure rather than failure of the tissue energy state. Although diffusion abnormalities that appear during acute arterial insufficiency are virtually always associated with permanent parenchymal injury, there is far less experience with diffusion-weighted imaging in acute venous insufficiency so that it is not known whether the same association exists. The complete reversal of a diffusion abnormality without any associated lesion on T2-weighted or fluid-attenuated inversion-recovery images is unique in our experience. In over 200 cases of echo-planar imaging of patients with arterial ischemic disease, we have never encountered this combination. Although the defects revealed by diffusion-weighted imaging were similar in size and appearance, quantification of the apparent diffusion coefficient revealed consistent differences between the two lesions (Table). The region with more severe reduction in diffusion ($< 0.20 \times 10^{-5}$ cm^2/s) was associated with

Apparent diffusion coefficient before and after thrombolysis

MR Slice #	ROI	Pre-Thrombolysis		Post-Thrombolysis	
		Right	Left	Right	Left
10	Anterior frontal	0.78 ± 0.24	0.72 ± 0.20	0.66 ± 0.17	0.72 ± 0.23
	Frontal lesion	0.16 ± 0.23	0.73 ± 0.18	0.81 ± 0.11	0.71 ± 0.22
	Parietal lesion	0.33 ± 0.13	0.79 ± 0.15	0.69 ± 0.14	0.85 ± 0.26
12	Anterior frontal	0.82 ± 0.13	0.72 ± 0.11	0.64 ± 0.17	0.70 ± 0.28
	Frontal lesion	0.18 ± 0.28	0.80 ± 0.18	0.46 ± 0.26	0.73 ± 0.16
	Parietal lesion	0.30 ± 0.17	0.85 ± 0.17	0.74 ± 0.15	0.70 ± 0.16
14	Anterior frontal	0.88 ± 0.34	0.80 ± 0.18	0.75 ± 0.21	0.69 ± 0.12
	Frontal lesion	0.20 ± 0.27	0.92 ± 0.12	0.58 ± 0.21	0.64 ± 0.17
	Parietal lesion	0.59 ± 0.27	0.70 ± 0.18	0.54 ± 0.27	0.78 ± 0.16

Note.—All values are means of ROI with standard errors with units of $cm^2/sec \times 10^5$.

a localized abnormality on conventional imaging and was incompletely reversed, although the ultimate lesion, visible at 1-year follow-up, was far smaller than the lesion observed on T2-weighted and fluid-attenuated inversion-recovery images upon presentation and immediately after thrombolysis. The area with less severe reduction ($> 0.30 \times 10^{-5}$ cm^2/s) never developed any corresponding anatomic abnormality and appeared to reverse completely immediately after thrombolysis. This suggests, but certainly does not prove, that quantitative apparent diffusion coefficients rather than diffusion defect volume will be more useful for establishing a threshold for permanent neurologic injury.

Perfusion-weighted imaging, performed with bolus injection of a paramagnetic contrast agent, can be used to derive maps of relative cerebral blood volume and the relative mean transit time. There is, at the present time, no generally applicable MR imaging method for quantifying regional cerebral blood flow, as this would require an arterial input function analogous to that obtained for positron-emission tomography. Perfusion-weighted imaging revealed widespread prolongation of the mean transit time while intradural pressures were elevated and the patient was symptomatic. There was prompt reversal of the delays in mean transit time after thrombolysis when pressures returned to normal, and the patient improved symptomatically. Somewhat surprisingly, there was no definite localized alteration of cerebral blood volume. In the absence of quantitative measurements of regional cerebral blood flow, no statement can be made regarding changes in total blood flow to the cerebral hemispheres after thrombolysis. Without this quantification, the role of perfusion-weighted imaging is restricted to the ability to recognize a significant perfusion abnormality and, perhaps, the ability to measure the volume of brain that is exposed to the altered perfusion.

The optimal management of dural sinus thrombosis requires a noninvasive method for identifying those patients in whom a more aggressive approach with thrombolysis is preferred over conservative management. Clinical signs at presentation do not correlate well with subsequent course or outcome. Determining intrasinus pressure may be a better discriminator but can be relatively invasive and its value for predicting outcome is unknown. Owing to the results of this single patient with superior sagittal and lateral sinus thrombosis, it appears that diffusion- and perfusion-weighted imaging may correlate well with both clinical course and intrasinus pressure, adding complementary information and potentially providing a noninvasive method of identifying those patients with dural sinus thrombosis who are candidates for immediate thrombolysis. Obviously, a single case cannot be used to develop guidelines for managing DST and many more cases correlating echo-planar MR imaging with intrasinus pressures and clinical outcome of patients with DST will be necessary to define the general applicability and limitations of the technique. The reversibility of the findings imply, however, that the technique will be well-suited to triaging patients for more aggressive management when the spectrum of abnormalities and their correlation with intrasinus pressures are better understood. Studies in animal models of DST could facilitate this understanding by providing a controlled situation in which to establish the relationship between intradural sinus pressure and echo-planar imaging. Whether measurement of apparent diffusion coefficients, diffusion defect volume, the volume with mean transit time delay, or even cerebral blood flow would be the most useful parameters for ascertaining the need for intervention is unknown and only systematic analysis of more patients and of animal models can yield that information.

References

1. Tsai FY, Wang AM, Matovich VB, et al. **MR staging of acute dural sinus thrombosis. Correlation with venous pressure measurements and implications for treatment and prognosis.** *AJNR Am J Neuroradiol* 1995;16:1021–1029
2. Di Ricco C, Iannelli A, Leone G, Moschini M, Valori VM. **Heparin-urokinase treatment of an aseptic dural sinus thrombosis.** *Arch Neurol* 1981;38:431–435

3. Tsai FY, Higashida RT, Matovich V, Alfieri K. **Acute thrombosis of the intracranial dural sinus: direct thrombolytic treatment.** *AJNR Am J Neuroradiol* 1992;13:1137–1141
4. Smith TP, Higashida RT, Barnwell SL, et al. **Treatment of dural sinus thrombosis by urokinase infusion.** *AJNR Am J Neuroradiol* 1994;15:801–807
5. Horowitz M, Purdy P, Unwin H, et al. **Treatment of dural sinus thrombosis using catheterization and urokinase.** *Ann Neurol* 1995;38:58–67
6. Rael JR, Orrison WW, Baldwin N, Sell J. **Direct thrombolysis of superior sagittal sinus thrombosis with coexisitng intracranial hemorrhage.** *AJNR Am J Neuroradiol* 1997;18:1238–1242
7. Ameri A, Bousser MG. **Cerebral venous thrombosis.** *Neurol Clin* 1992;10:87–111
8. Le Bihan D. **Molecular diffusion nuclear magnetic resonance imaging.** *Magn Res Q* 1991;7:1–30
9. Pierpaoli C, Righini A, Linfante I, Tao-Cheng JH, Alger JR, Ci Chiro G. **Histopathologic correlates of abnormal water diffusion in cerebral ischemia: diffusion-weighted MR imaging and light and electron microscopic study.** *Radiology* 1993; 189:439–448
10. Herscovitch P, Markham J, Raichle ME. **Brain blood flow measured with intravenous $H_2{}^{15}O$ I. Theory and error analysis.** *J Nucl Med* 1983;24:782–789